Genomics, Proteomics & Bioinformatics, 2024, **22(2)**, qzae033
https://doi.org/10.1093/gpbjnl/qzae033
Advance access publication: 18 April 2024
Original Research

Proteomic Stratification of Prognosis and Treatment Options for Small Cell Lung Cancer

Zitian Huo [1,2,3,#], Yaqi Duan [1,2,3,#], Dongdong Zhan [4,#], Xizhen Xu [5,#], Nairen Zheng [6,#], Jing Cai [7], Ruifang Sun [8], Jianping Wang [6,9], Fang Cheng [4], Zhan Gao [6], Caixia Xu [6], Wanlin Liu [6], Yuting Dong [1,2], Sailong Ma [1,2,3], Qian Zhang [1,2], Yiyun Zheng [1], Liping Lou [1], Dong Kuang [1], Qian Chu [5], Jun Qin [4,6], Guoping Wang [1,2,3,*], Yi Wang [6,*]

[1]Institute of Pathology, Tongji Hospital, Tongji Medical College, Huazhong University of Science and Technology, Wuhan 430030, China
[2]Department of Pathology, School of Basic Medicine, Tongji Medical College, Huazhong University of Science and Technology, Wuhan 430030, China
[3]National Health Commission Key Laboratory of Respiratory Diseases, Tongji Hosptial, Tongji Medical College, Huazhong University of Science and Technology, Wuhan 430030, China
[4]Beijing Pineal Diagnostics Co., Ltd., Beijing 102206, China
[5]Department of Oncology, Tongji Hospital, Tongji Medical College, Huazhong University of Science and Technology, Wuhan 430030, China
[6]State Key Laboratory of Proteomics, Beijing Proteome Research Center, National Center for Protein Sciences (Beijing), Beijing Institute of Lifeomics, Beijing 102206, China
[7]Institution of Pathology, The First Affiliated Hospital of Henan University, Kaifeng 475001, China
[8]Department of Tumor Biobank, Shanxi Cancer Hospital, Taiyuan 030013, China
[9]Chongqing Key Laboratory of Big Data for Bio Intelligence, School of Bioinformation, Chongqing University of Posts and Telecommunications, Chongqing 400065, China

*Corresponding authors: wangyi@ncpsb.org.cn (Wang Y), wanggp@hust.edu.cn (Wang G).
#Equal contribution.

Handling Editor: Minjia Tan

Abstract

Small cell lung cancer (SCLC) is a highly malignant and heterogeneous cancer with limited therapeutic options and prognosis prediction models. Here, we analyzed formalin-fixed, paraffin-embedded (FFPE) samples of surgical resections by proteomic profiling, and stratified SCLC into three proteomic subtypes (S-I, S-II, and S-III) with distinct clinical outcomes and chemotherapy responses. The proteomic subtyping was an independent prognostic factor and performed better than current tumor–node–metastasis or Veterans Administration Lung Study Group staging methods. The subtyping results could be further validated using FFPE biopsy samples from an independent cohort, extending the analysis to both surgical and biopsy samples. The signatures of the S-II subtype in particular suggested potential benefits from immunotherapy. Differentially overexpressed proteins in S-III, the worst prognostic subtype, allowed us to nominate potential therapeutic targets, indicating that patient selection may bring new hope for previously failed clinical trials. Finally, analysis of an independent cohort of SCLC patients who had received immunotherapy validated the prediction that the S-II patients had better progression-free survival and overall survival after first-line immunotherapy. Collectively, our study provides the rationale for future clinical investigations to validate the current findings for more accurate prognosis prediction and precise treatments.

Key words: Small cell lung cancer; Proteomics; Prognosis; Chemotherapy response; Immunotherapy.

Introduction

Small cell lung cancer (SCLC) is an exceptionally aggressive lung neuroendocrine neoplasm characterized by rapid tumor growth, early metastasis, and acquired chemo-resistance. Comprehensive whole-exome and whole-genome analyses have identified inactivation of *TP53* and *RB1* as the predominant genetic alterations in SCLC, occurring in > 98% of the patients [1,2]. Genomic analysis of 51 SCLC cases also found genetic alterations in the PI3K/AKT/mTOR pathway in 36% of the samples, with mutations in *PIK3CA* (6%), *PTEN* (4%), *AKT2* (9%), *AKT3* (4%), *RICTOR* (9%), and *mTOR* (4%) [3]. However, effective stratification markers and treatment targets for SCLC remain limited [4]. As a result, the overall survival (OS) of SCLC patients has seen no significant improvement despite numerous clinical trials of different chemotherapy schemes and biological agents over the past decades [5]. Moreover, a lack of biomarkers that help predict efficacy has also impeded SCLC patients from reaping significant benefits from immunotherapy [6]. Currently, the 5-year survival rate is approximately 20%–25% for limited-stage SCLC (LS-SCLC) and barely 1%–2% for extensive-stage SCLC (ES-SCLC), making SCLC one of the deadliest cancers.

Early studies based on cell line morphologies classified SCLC into classic subtypes that expressed higher neuroendocrine markers and variant subtypes that showed low or an absence of neuroendocrine features [7,8]. These characteristics were further observed in clinical samples [9,10]. Subsequently, SCLC was classified according to the expression of neuroendocrine transcription factors ASCL1 and/or NeuroD1 [11]. Additionally, POU2F3 expression was used to define a non-neuroendocrine, tuft cell variant of SCLC [12]. And although YAP1 was proposed as a potential subtype marker for the remaining unclassified SCLC cases

Received: 17 April 2023; **Revised:** 24 October 2023; **Accepted:** 22 January 2024.

[3], it has yet to be confirmed [13]. Recently, re-analyzing previously published transcriptomic data classified SCLC into four subtypes [14]; in addition to the previously identified subtypes with the ASCL1 (SCLC-A), NeuroD1 (SCLC-N), and POU2F3 (SCLC-P) signatures, a new subtype (SCLC-I) characterized by the expression of inflammation gene signatures was uncovered.

In IMpower133, a global phase I/III, double-blind, randomized, placebo-controlled trial, atezolizumab (anti-PD-L1) was added to carboplatin + etoposide for ES-SCLC. SCLC-I patients were reported to experience the greatest benefit from this combined immunotherapy and chemotherapy. In the randomized, controlled, open-label, phase III CASPIAN trial, first-line durvalumab plus platinum–etoposide also significantly improved OS in patients with ES-SCLC *vs*. a clinically relevant control group [15]. Additionally, cisplatin treatment of SCLC-A patient-derived xenografts (PDXs) induced intratumoral shifts toward SCLC-I [16]. These analyses suggest that the SCLC-I subtype might be the right candidate for immunotherapy. Therapeutic vulnerabilities were also identified for each subtype, including to inhibitors of PARP (SCLC-P), Aurora kinases (SCLC-N), or BCL-2 (SCLC-A) [16]. More recently, single-cell RNA sequencing (scRNA-seq) and imaging techniques have further revealed the heterogeneity and tumor microenvironment (TME) of SCLC [16]. Monocytes/macrophages appear to play a profibrotic and immunosuppressive role in SCLC TME. SCLC-N shows less immune infiltrate and greater T cell dysfunction than SCLC-A. More importantly, most SCLC cases share a small PLCG2-high subpopulation, which is linked to metastasis and poor prognosis.

While subtyping based on genomic and transcriptomic analyses has greatly improved our understanding of SCLC, the resulting subtypes correlate poorly with clinical outcomes. In contrast, subtyping with proteomics has revealed its exceptional clinical potential for more accurate predication of prognosis, chemo-sensitivity, and treatment targets for myriad cancers including stomach [17,18], liver [19,20], ovarian carcinoma [21], colorectal cancer [22], and non-small cell lung cancer (NSCLC) [23,24]. Here, we reported a proteomic subtyping model derived from a discovery dataset containing 75 surgically resected formalin-fixed, paraffin-embedded (FFPE) samples. The model was then validated in an independent cohort of 52 FFPE biopsy samples. The subtypes based on our proteomic model correlated well with clinical information including OS, and also allowed subtype-specific nomination of drug targets in SCLC. In addition, analysis of another 52 samples from patients who received immunotherapy allowed us to validate the finding that one particular proteimic subtype is an immune responsive subtype.

Results

Limited predictive power of SCLC staging and classification systems

In an effort to develop a more reliable SCLC subtyping system, we first analyzed the 75 surgically resected FFPE SCLC samples as shown in **Figure 1A**. Key clinical characteristics of the patients in the discovery cohort are presented in Figure 1B, with their detailed clinical and pathological data provided in Table S1. Of the 75 cases, 62 (82.7%) were LS-SCLC and 13 (17.3%) were ES-SCLC according to the Veterans Administration Lung Study Group (VALG) definition. Based on the tumor–node–metastasis (TNM) staging system, 13 (17.3%), 19 (25.3%), 28 (37.3%) and 13 (17.3%) cases were categorized as stage I, II, III, and IV, respectively. At the end of follow-up, 31 (41.3%) patients survived, with a median OS time of 2.78 ± 0.25 years. The statistically significant univariate prognostic factors included age (log-rank test, $P = 0.035$), gender (log-rank test, $P = 0.0085$), and lymph node metastasis (LNM) (log-rank test, $P = 0.01$) (Figure S1).

When the predictive value of the current staging systems (including VALG and TNM) were examined against actual prognosis of SCLC patients, their limitations became clear (Figure 1C). In fact, only TNM I patients had significantly better OS than those of TNM IV (log-rank test, $P = 0.04$) (Figure 1C). Immunohistochemistry (IHC) was used to examine the expression of ASCL1, NeuroD1, and YAP1 in the samples, and positive rates of 81.3% (61/75), 20% (15/75), and 4% (3/75), were obtained respectively. Of all cases, 11 were double-positive for ASCL1 and NeuroD1 (Figure S2; Table S1). However, classification based on ASCL1/NeuroD1 expression did not correlate with OS differences in patients either (Figure 1C), although the NeuroD1^{+}/ASCL1^{-} subtype showed better but not statistically significant prognosis (log-rank test, $P = 0.561$).

Proteomics stratifies SCLC into subtypes that correlate with clinical outcomes

Since the current SCLC staging and classification systems failed to make a satisfactory prediction, we carried out a proteomic study using these 75 samples by label-free quantitative mass spectrometry (MS) (Figure 1A). We detected a total of 7028 gene products of high confidence from 75 samples, with 2957 proteins identified in more than 50% samples. The protein identities and relative abundances of each case, designated as fraction of total (FOT) [25], are provided in Table S2. To develop a robust classification model, we first selected the top 1100 most abundant proteins detected from each sample, which yielded a dataset of 3460 proteins; then the 445 proteins that were detected in at least 8 samples (> 10%) with the coefficient of variation (CV) greater than 1.9 were used for non-negative matrix factorization (NMF) consensus clustering (Table S3). NMF clustering yielded three subgroups, namely S-I ($n = 28$, 37%), S-II ($n = 20$, 27%), and S-III ($n = 27$, 36%) with the maximum average silhouette of 0.83 (**Figure 2A**). Importantly, these proteomic subtypes correlated well with OS prognosis. Patients in S-I had the best OS with a 5-year OS probability of 75%, whereas S-III had the worst survival with only 3.7% of 5-year OS (log-rank test, $P < 0.001$) (Figure 2B). A multivariate Cox analysis confirmed that the proteomic subtype was an independent prognostic factor [S-I *vs*. S-III: hazard ratio (HR) = 4.73, 95% confidence interval (CI) = 1.81–12.4, Cox P value = 0.002] after adjusting for TNM stage, VALG stage, and other covariates including chemotherapy, age, gender, LNM status, and smoking history (Figure S3). These data indicate that proteomics-based subtyping is superior in OS prognosis.

The proteomic subtypes show different benefit of chemotherapy on prognosis

The platinum agent (cisplatin or carboplatin) and etoposide-based combination chemotherapy is the standard care for SCLC patients after surgery, although the percentage of patients who actually benefit from such care is quite small

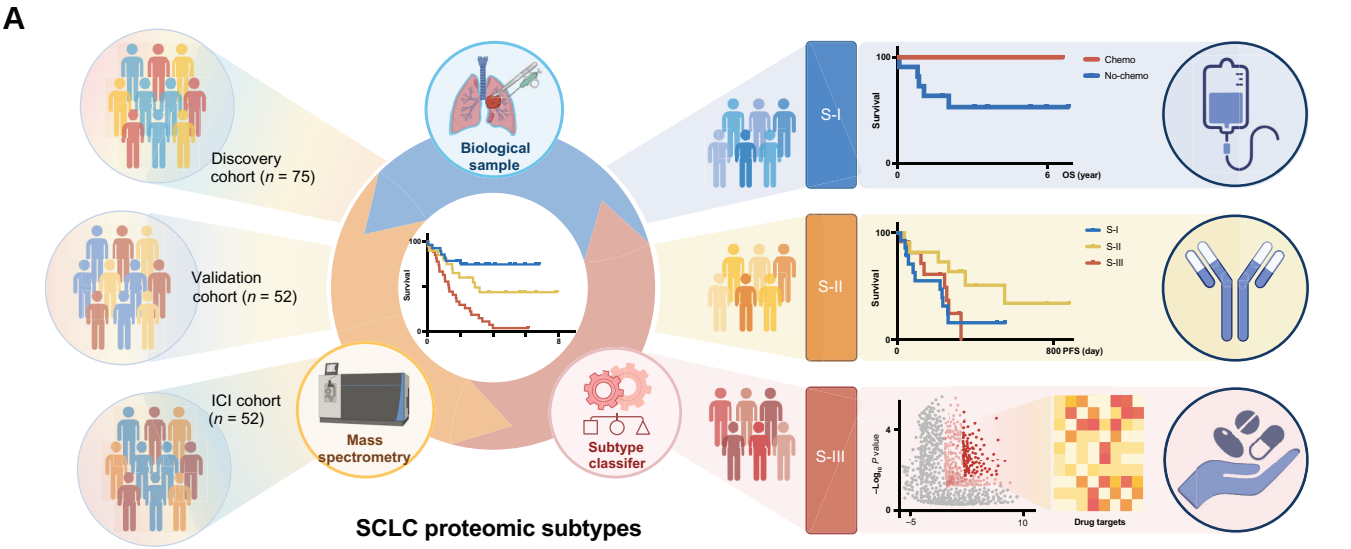

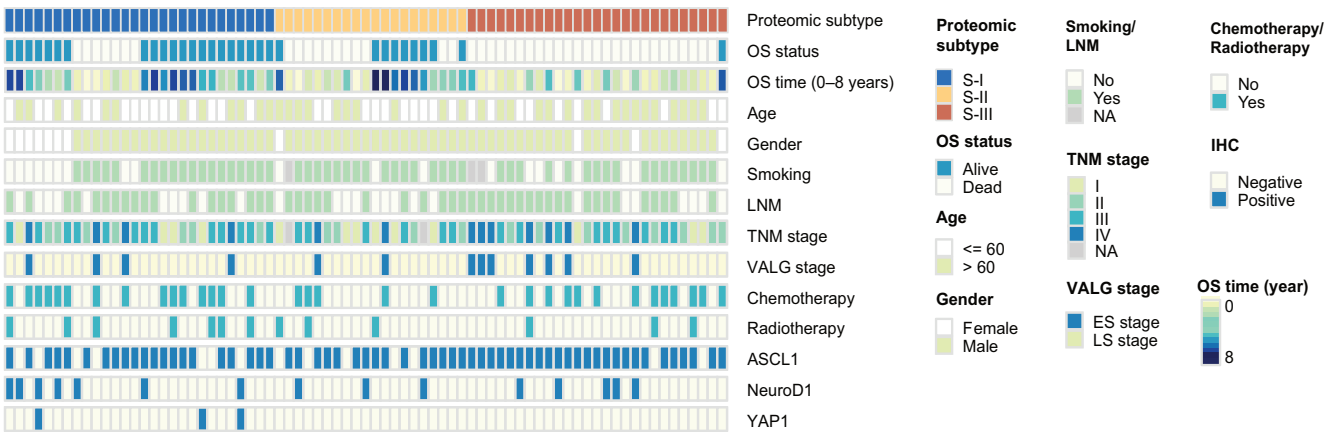

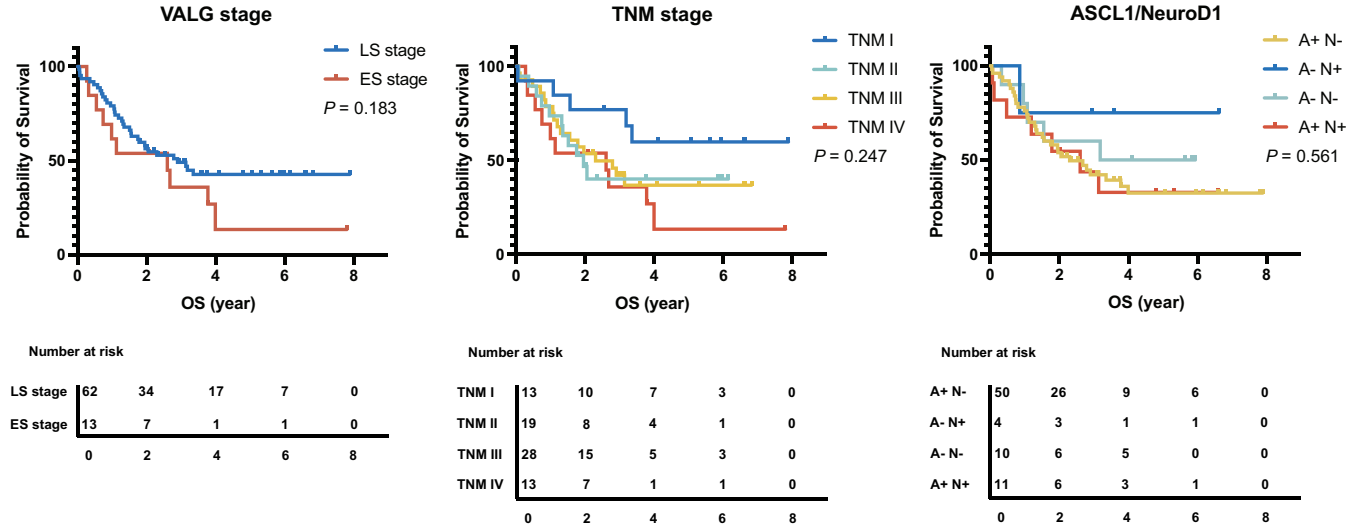

Figure 1 Study design and key clinical characteristics of the SCLC patients from the discovery cohort
A. A flowchart of our study scheme. **B**. Clinical characteristics of the patients from the discovery cohort. **C**. The Kaplan–Meier plots showing the limited predictive values on patient OS of the VALG, TNM, and ASCL1/NeuroD1 staging and classification methods. SCLC, small cell lung cancer; TNM, tumor–node–metastasis; VALG, Veterans Administration Lung Study Group; OS, overall survival; PFS, progression-free survival; ICI, immune checkpoint inhibitor; LNM, lymph node metastasis; LS, limited stage; ES, extensive stage.

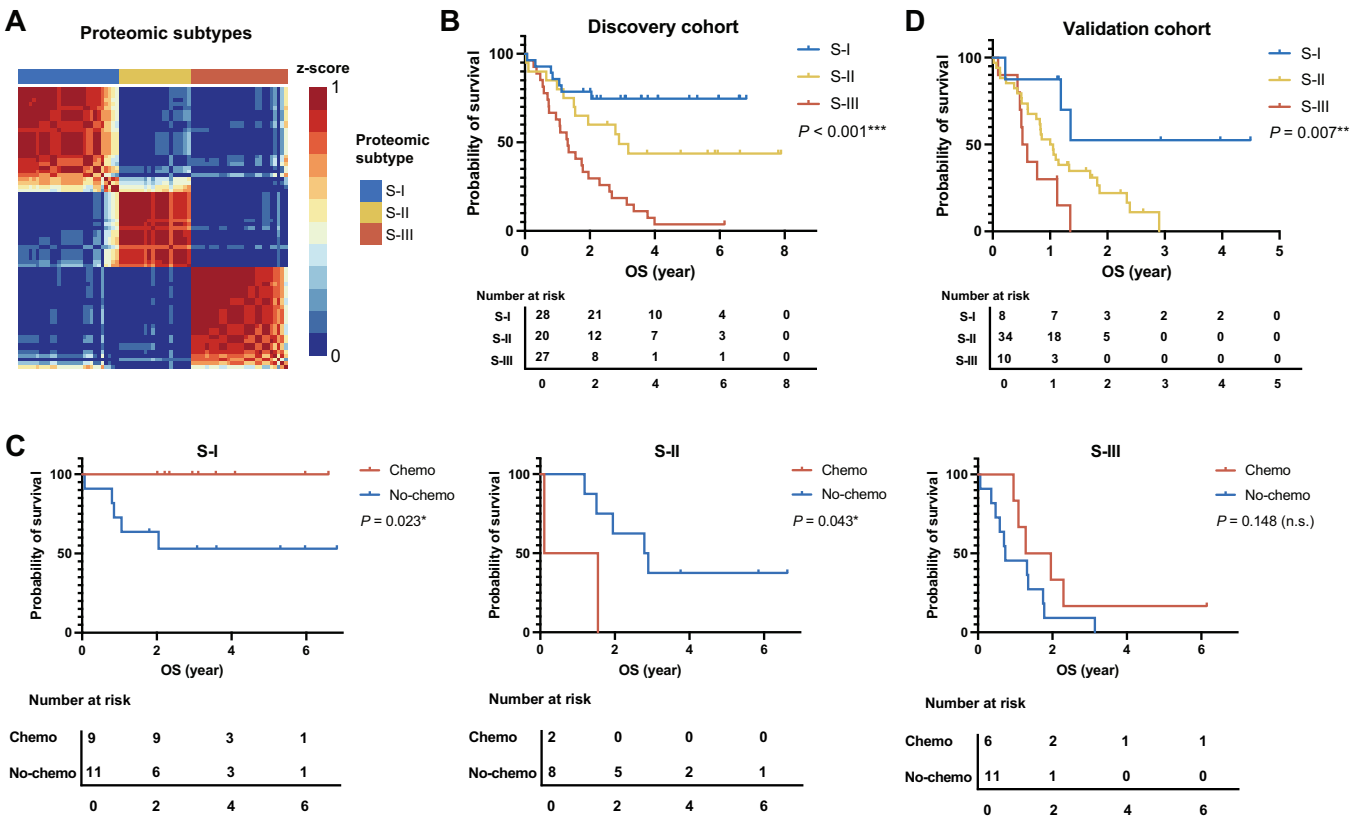

Figure 2 Proteomics stratifies SCLC into subtypes that correlate with clinical outcomes

A. NMF clustering yielded three subgroups in SCLC in the discovery cohort. **B**. The three subtypes based on proteomic profiling were associated with different clinical outcomes. **C**. The three proteomic subtypes exhibited different responses to chemotherapy. **D**. The predictive classifier model showing the prognosis trend similar to the discovery cohort. In the validation cohort, biopsy samples were obtained from the First Affiliated Hospital of Henan University, China. *P* values were determined by log-rank test (*, $P < 0.05$; **, $P < 0.01$; ***, $P < 0.001$; n.s., not significant). NMF, non-negative matrix factorization.

[26]. In our dataset, approximately half of the patients (n = 33, 44%) underwent chemotherapy. Considering the impact of TNM I and IV on prognosis mentioned earlier, we included only TNM II and III patients for chemo-sensitivity analysis. As shown in Figure 2C, chemotherapy exhibited different impacts on prognosis for the three proteomic subtypes. The S-I subtype benefited most significantly from chemotherapy (log-rank test, $P = 0.023$), with all patients who received chemotherapy still alive by the end of the study. The S-II subtype appeared to have worse prognosis (log-rank test, $P = 0.043$). The S-III subtype had the worst prognosis and was chemo-insensitive (log-rank test, $P = 0.148$). In summary, our proteomic SCLC subtyping could stratify patients into three distinct subtypes that are more clinically relevant. The S-I subtype is chemo-sensitive with the best OS. S-II has medium OS where chemotherapy might be detrimental. S-III has the poorest prognosis and is insensitive to chemotherapy, suggesting that S-III patients have the greatest need for new therapies.

To facilitate the validation of the subtyping in the independent external dataset, we developed a random forest (RF) classifier with the discovery dataset. The top 500 most abundant proteins detected in each sample were aggregated for differential expression analysis. The resulted 58 signature proteins [fold change (FC) > 1.5; adjusted *t*-test, $P < 0.05$] with high identification frequencies (detected in more than 25% of the samples) were used as input (predictor variables) (Table S4). We trained a RF classifier with a 10-fold cross-validation in the discovery dataset. Based on the 58 features, the predictive classifier model yielded a 90.8% accuracy for the discovery dataset. We collected 52 SCLC biopsy samples from another center (the First Affiliated Hospital of Henan University, Kaifeng, China) as an independent validation dataset. The corresponding clinical information of these samples is summarized in Table S5. This subset included 12 female and 40 male patients, with an OS time ranging from 0.019 to 4.493 years. The 2-year survival rate was 15.4% (8/52) and the 3-year survival rate was 3.8% (2/52). Proteomic analysis was performed on the 52 biopsy samples. The results are listed in Table S6. When the RF classifier was applied to the validation dataset, the predicted S-I, S-II, and S-III subtypes contained 8, 34, and 10 cases, respectively. The prognosis trend was consistent with that of the discovery cohort, with 1-year survival rates of 87.5%, 52.9%, and 30.0% and 2-year survival rates of 37.5%, 14.7%, and 0% for S-I, S-II, and S-III, respectively. Kaplan–Meier analysis illustrated that the OS varied significantly among the three subtypes (log-rank test, $P = 0.007$) (Figure 2D). Thus, the proteomic subtyping model derived from surgical samples could be validated with biopsy samples from an independent cohort.

Differential signature proteins and enriched biological processes in proteomic SCLC subtypes

To investigate the proteomic features of SCLC subtypes, we selected significantly altered proteins by comparing their expression in each subtype to the other subtypes (FC > 3 for S-I

and S-II or FC > 10 for S-III; Wilcox test, $P < 0.05$). As a result, 206, 162, and 126 subtype-specific proteins for S-I, S-II, and S-III, respectively, were designated as significantly altered proteins (**Figure 3A**; Table S7). Functional enrichment using Metascape showed that the most distinct subtype was S-II, which was significantly enriched in NABA core matrisome, interferon signaling, and immune-related processes/responses (adjusted P values were between 1×10^{-17} and 1×10^{-8}) (Figure 3B). In the regulation of immune functions, major histocompatibility complex class I (MHC-I) molecules play an important role in cell-mediated immunity by presenting tumor antigens to $CD8^+$ T cells and enabling cytotoxic T cells to recognize and eliminate tumor cells. Antigen presenting cells (APCs) such as B cells, dendritic cells (DCs), and monocytes/macrophages express major histocompatibility complex class II (MHC-II) molecules and present antigenic peptides to $CD4^+$ helper T cells. Here, we found that the MHC-I molecules (including HLA-A, HLA-B, HLA-C, HLA-E, and HLA-F) but not the MHC-II molecules (including HLA-DQA1, HLA-DQB1, HLA-DRA, HLA-DRB1, and HLA-DRB5) were expressed at higher levels in S-II than in the other two subtypes ($P < 0.05$, rank sum test between two groups and Kruskal-Wallis rank sum test for all; Figure 3C and D). Moreover, TAP1, TAP2, and TAPBP were also highly expressed in S-II. TAP1 and TAP2 are members of the superfamily of ATP-binding cassette (ABC) transporters that shuttle various molecules across extra-cellular and intracellular membranes. The ATP-loaded TAP1–TAP2 complex mediates unidirectional translocation of peptide antigens from the cytosol to endoplasmic reticulum (ER) for their loading onto MHC-I molecules [27]. TAPBP is a transmembrane glycoprotein that mediates interactions between newly assembled MHC-I molecules and TAP proteins, and is required for the transport of antigenic peptides across ER membrane [28]. Thus, the S-II subtype is characterized by an enrichment of factors involved in antigen presentation.

The S-I subtype appeared to be marginally enriched in proteins functioning in transport, membrane trafficking, and RNA metabolic processes (adjusted P values of 1×10^{-4}–1×10^{-2}). Detailed analysis identified ubiquitin-mediated proteolysis in cell cycle control, including the anaphase promoting complex (ANAPC1, ANAPC13, and ANAPC4) and COPS9 signalosome components (COPS3 and COPS7B) as well as NEDD8. DNA repair and DNA replication proteins, including MSH3, LIG1, POLE3, RFC3, ORC2, and ATM, were also enriched (Table S7). After adjusting for P values, Metascape analysis could not identify significantly enriched biological processes for S-III. Manual inspection showed that proteins in chromatin organization/transcription regulation as well as various enzymes were enriched (Table S7). Among them were proteins mediating chromatin assembly and telomere maintenance (CHAF1A, TERF2, and TOX4), transcription coactivators (*e.g.*, ATAD2, ZNF516, PHF6, PHF8, MED6, TAF5, and TAF), and transcription corepressors (*e.g.*, TBL1X, TBL1Y, CHD8, ATXN2, and SPEN). It appears that mis-regulation in chromatin structure and transcription may profoundly impact an array of biological processes, which the Metascape algorithm might have failed to identify.

The S-II patients have the best immunotherapy responses in SCLC

Aforementioned analyses suggest that S-II is an inflamed SCLC subtype in nature, which may benefit from immunotherapy. To test this hypothesis, we collected another 52 real-world FFPE biopsy or surgery samples from ES-SCLC patients who received immune checkpoint inhibitors (ICIs; including sintilimab, toripalimab, durvalumab, camrelizumab, tislelizumab, and atezolizumab), termed as the ICI cohort. Among these samples, 37 were treated with combined immunotherapy with chemotherapy as a first-line treatment, and 49 were from biopsy (**Figure 4A**; Table S8). We classified these samples using the model derived from the discovery dataset (Table S9) into S-I (23 patients), S-II (13 patients), and S-III (16 patients). We specified an ICI progression-free survival (ICI-PFS) as the duration between the time when the first immunotherapy was applied, and progressive disease (PD) was determined by clinical standards. As shown in Figure 4B and C, the ICI-PFS of the S-II patients with first-line ICIs rather than > first-line ICIs was longer than that of S-III (log-rank test, $P = 0.038$) and S-I (log-rank test, $P = 0.056$). Moreover, when the Kaplan–Meier plots of the S-II patients in the ICI cohort, the discovery cohort (WH-S-II, no immunotherapy), and the validation cohort (HN-S-II, no immunotheray) were compared, the S-II patients treated with ICIs achieved better OS (ICI cohort *vs.* discovery cohort: $P = 0.03$; ICI cohort *vs.* validation cohort: $P < 0.0001$; log-rank test) (Figure 4D). Together, these analyses demonstrate the values of stratifying patients for immunotherapy, and suggest that immunotherapy could significantly improve the OS of SCLC patients, particularly for those in the S-II subtype.

Potential drug repurposing targets for S-III subtype patients

Since patients in the S-III subtype had the worst OS and did not benefit from chemotherapy, they were the most in need of new therapeutic options. We selected specifically overexpressed proteins in S-III compared with S-I and S-II and investigated their feasibility as potential drug repurposing targets. We first identified previously investigated actionable drug targets and found that at least one target among EGFR, AURKB, BCL-2, and EZH2 was highly expressed in 77.8% (21/27) of the S-III patients. Drugs targeting AURKB, BCL-2, or EZH2 are currently in various stages of clinical development and have shown promising results for treating certain cancers [29,30]. Many kinases, phosphatases, transporters, ubiquitin–proteasome system (UPS) proteins, and other enzymes were overexpressed in S-III, accounting for nearly 1/3 of all specifically overexpressed proteins in S-III. Proteins that regulate necroptosis, including MLKL, TRAF2, and RIPK1, are also potential targets [31]. Their druggability needs to be further investigated. An overview of the potential drug repurposing targets for each individual patient is shown in **Figure 5**.

Discussion

While genomic and transcriptomic analyses have greatly improved our understanding of SCLC tumorigenesis, their values in identifying effective stratification markers and therapeutic targets are limited. In this retrospective proteomic analysis, we showed that proteomics alone could stratify SCLC for prognosis and chemo-sensitivity. Since most SCLC tumors are non-resectable when diagnosed, we validated our proteomic subtyping using biopsy samples from an independent center, expanding the clinical utility of our proteomic subtyping method. Our analysis showed that all S-I patients

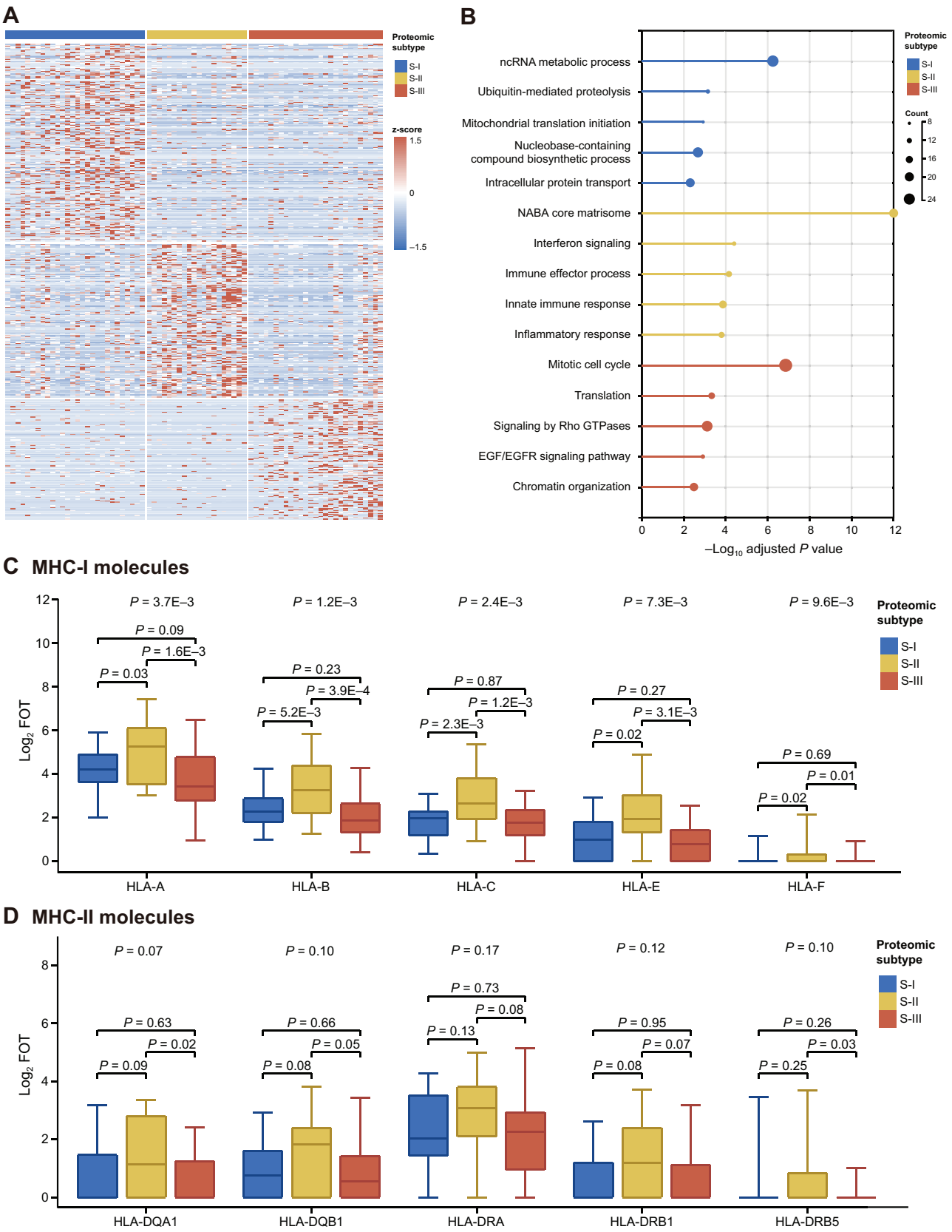

Figure 3 Differential signature proteins and enriched biological processes in proteomic SCLC subtypes

A. Heatmap of signature proteins in each subtype. **B**. Metascape functional enrichment analysis identified different biological processes or pathways activated in the three subtypes. **C**. and **D**. The MHC-I (C) rather than MHC-II (D) molecules were highly expressed in S-II compared with S-I and S-III. *P* values were determined by rank sum test between two groups and Kruskal-Wallis rank sum test for all. MHC-I, major histocompatibility complex class I; MHC-II, major histocompatibility complex class II; FOT, fraction of total.

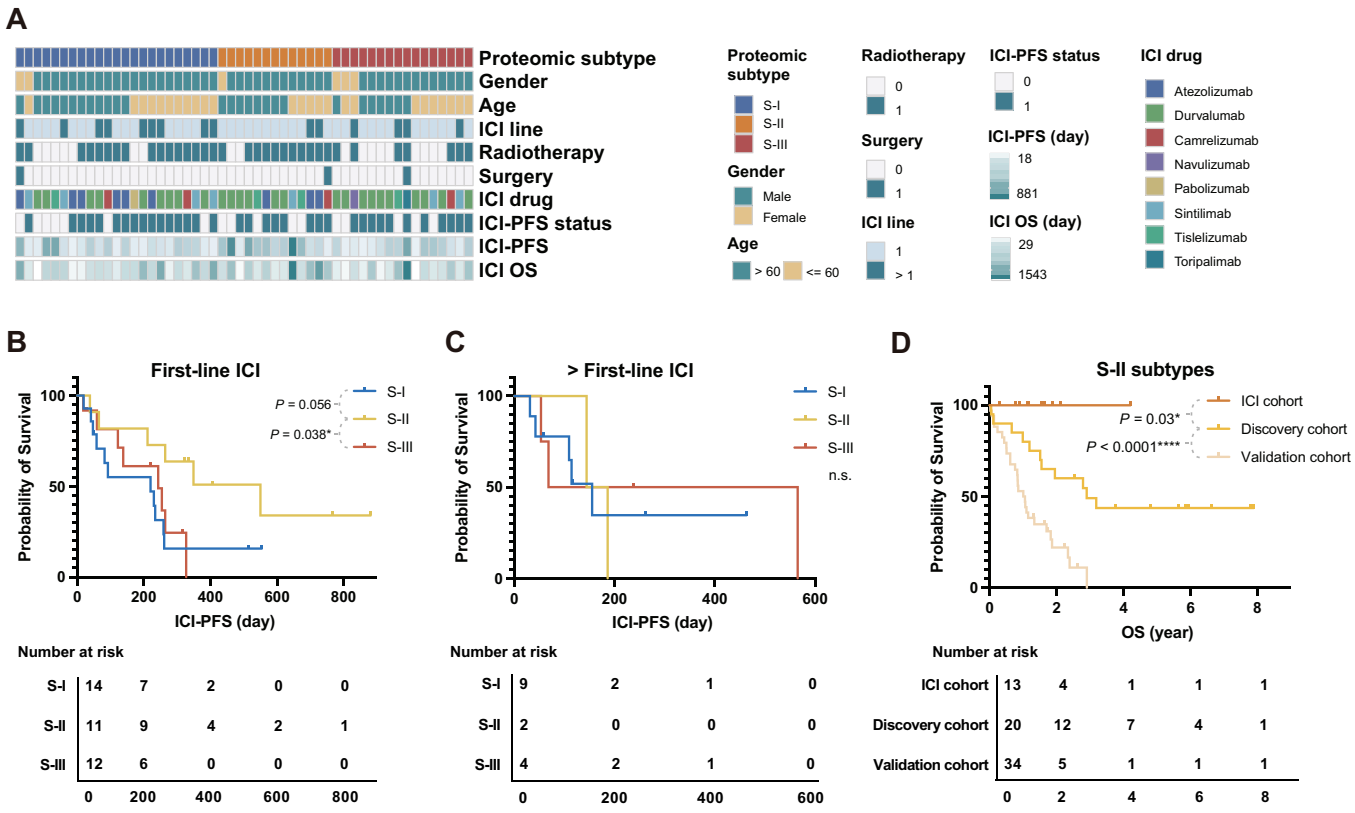

Figure 4 The S-II subtype patients are more likely to benefit from immunotherapies
A. The clinical characteristics of the patients from the ICI cohort. **B**. and **C**. In the ICI cohort, the S-II patients had the best PFS time when receiving first-line immunotherapy (B) but showed no statistically obvious difference compared with S-I/S-III patients when receiving second-line immunotherapy (C). **D**. In all S-II patients, patients after immunotherapy had better OS than those without immunotherapy. S-II patients in the ICI cohort and S-II patients who did not receive immunotherapy in the discovery and validation cohorts were used for analysis. *P* values were determined by log-rank test (*, $P < 0.05$; ****, $P < 0.0001$; n.s., not significant).

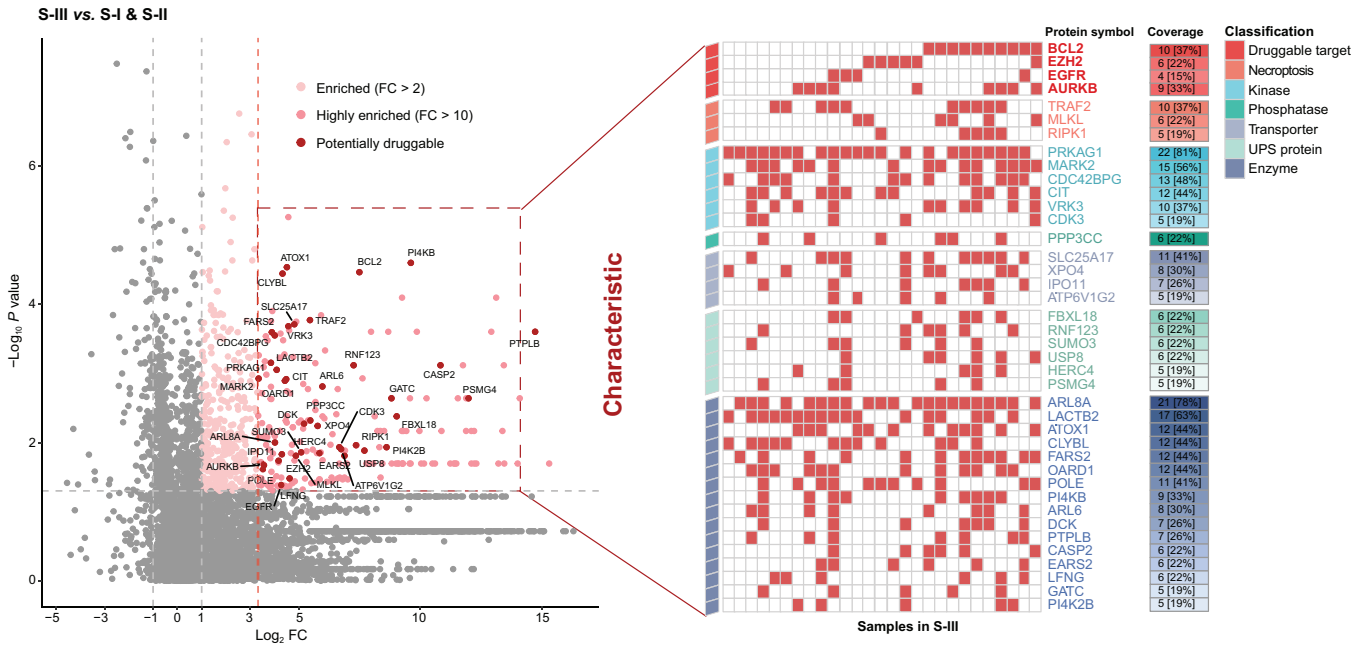

Figure 5 The atlas of potential drug targets for individual patients in S-III
FC, fold change; UPS, ubiquitin–proteasome system.

in the discovery cohort who received chemotherapy were alive by the end of the study, confirming the suitability of chemotherapy as first-line treatment option for these patients. Antigen presentation and other immune responses were enriched in S-II, suggesting that ICIs may be a viable choice for S-II patients. We validated this prediction in a third independent group of patients that received immunotherapy as the first-line treatment. Notably, a previous transcriptomic study also defined an "inflamed" SCLC subtype (SCLC-I) [15] which was characterized by high expression of genes related to HLAs and experienced greatest benefit from the addition of anti-PD-L1 to chemotherapy [15]. Our proteomic subtyping thus may provide value in guiding SCLC treatment.

Since neither PD-L1 expression nor TMB is a reliable biomarker for the prediction of immunotherapy response in clinical trials such as IMpower133 and CheckMate-032, other biomarkers are in great need. Our analysis showed that patients in the S-II subtype may benefit from the immunotherapy. Although they were mostly ES-SCLC and lost the oppotunity for surgery, the 2-year survival rate of the S-II patients with immunotherapy reached over 30%, much better than the other subtypes. In other clinical trials (*e.g.*, ASTRUM-005), the median PFS was generally less than 6 months [32], which was similar to that of S-I/S-III patients in our study. However, the median PFS reached around one year for the S-II subtype here. It will be important to investigate in a prospective trial to determine whether the S-II subtype could serve as a new predictive biomarker for guiding SCLC immunotherapy.

Mechanisms of immune resistance vary [33]. MHC-I molecules were generally expressed at low levels in the SCLC tumor cells, resulting in low antigen presentation. In addition, tumor cells can also secrete factors to inhibit antigen presenting cells. About 50% of patients with SCLC have almost no T cell infiltration, and there are also suppressive immune cells in the immune microenvironment of SCLC. In our study, S-II subtype had higher MHC-I molecules along with other proteins in antigen presenting. Interferon gamma signaling was also enriched in S-II. Thus, S-II may be the immune hot subtype while S-I and S-III were the cold ones.

Among proteins and pathways as potential drug targets for the S-III subtype, BCL-2, EZH2, ARUKB, and EGFR are actionable drug targets that have been at various stages of clinical trials. Among them, EZH2 was identified as an upstream regulator in the SLFN11 axis that mediates acquired chemoresistance in an *in vitro* PDX model [34]. Food And Drug Administration (FDA) has recently approved the EZH2 inhibitor tazemetostat for treating epithelioid sarcoma [35]. Interestingly, EZH2 is a negative regulator of MHC-I molecules, and inhibiting EZH2 could enhance antigen presentation and circumvent anti-PD-1 resistance [36]. Although EGFR tyrosine kinase inhibitors (EGFR-TKIs; such as gefitinib) are not effective in a SCLC clinical trial [37], the identification of a subgroup of patients with EGFR overexpression suggest an alternative approach by using EGFR antibody. Notably, EGFR antibody has been approved as first-line treatment option for KRAS wild-type, EGFR-overexpressing colon cancer patients [38]. BCL-2 family proteins comprise the sentinel network that regulates mitochondrial and intrinsic apoptotic responses. Previous studies of a BCL-2 inhibitor fell short of expectations in SCLC clinical trials [39]. A possible explanation is that patients in the trial were not screened for BCL-2 expression. Interestingly, the SCLC-A transcriptomic subtype [15], which had higher expression of BCL-2, was found to be sensitive to multiple BCL-2 inhibitors in an *in vitro* study. Recently, the single target BCL-2 inhibitor venetoclax, which was approved by the FDA for acute myeloid leukemia and chronic lymphocytic leukemia [40], showed therapeutic effect on multiple PDXs of SCLC [41]. AURKB is a mitotic protein kinase. Phase I/II clinical studies of its inhibitor alisertib have demonstrated increased antitumor effects in various hematologic malignancies and solid tumors [42].

In addition, our proteomic data suggest that necroptosis regulators including MLKL, TRAF2, and RIPK1 may be investigated as potential therapeutic targets for SCLC. Necroptosis causes cellular swelling and plasma membrane collapse, which may lead to the release of intra-cellular biomolecules including damage-associated molecular patterns (DAMPs) and cytokines. These molecules can perform immunological functions such as chemotaxis, phagocytosis, and immune cell activation [43]. Although initial attraction of antigen presentation cells such as macrophages and DCs by DAMPs/cytokines could recruit $CD8^+$/$CD4^+$ T cells for immune activation in early stage, the recruitment of myeloid-derived suppressor cells (MDSCs) and tumor-associated macrophages (TAMs) at later stages could lead to immune suppression [44]. The effects of necroptosis proteins on tumors are cancer dependent. Cytokines released by necroptotic cancer cells can promote tumor angiogenesis, proliferation, and metastasis. For instance, high expression of RIPK1 was linked to metastasis in breast cancer [45] and poor survival in glioblastoma [46], but was a good prognostic indicator in head and neck cancer [47]. High MLKL expression correlated positively with good prognosis in colorectal cancer [48], high-risk human papillomavirus (HR-HPV) cervical cancer [49], ovarian cancer [50], and pancreatic adenocarcinoma [51], but negatively with breast cancer [52], cervical squamous cell carcinoma [53], and gastric cancer [54]. We found in this study a correlation between high expression of MLKL, TRAF2, and RIPK1 and the most malignant SCLC S-III subtype, suggesting that these proteins may represent good targets for treating SCLC.

The S-III subtype is also enriched for proteins involved in chromatin organization and transcriptional regulation. For example, CHAF1A, TERF2, and TOX4 can mediate chromatin assembly, protect chromosome ends, and regulate chromatin binding during DNA replication [55], metaphase [56], and transition to interphase [57], respectively. For transcriptional regulation, ATAD2 and ZNF516 act as transcription activators, promoting the expression of CCND1/MYC/E2F1 [58] or genes related to cellular response to replication stress [59], respectively. Moreover, PHF8 acts as a coactivator of ribosomal DNA (rDNA) transcription by activating polymerase I-mediated transcription of ribosomal RNA (rRNA) genes [60], while MED6 is a coactivator involved in the regulated transcription of nearly all RNA polymerase II-dependent genes [61]. These findings underline the importance of investigating dysfunctional chromatin organization in the development and treatment of SCLC.

Our study has some limitations. For example, our discovery cohort was relatively small compared with other omics studies, such as those of NSCLC. This is in part because most SCLC cases were detected at late stages without opportunity for surgery, so large-scale proteomic analysis of surgically resected samples was rare in the past. Moreover, our

proteomic stratification was different from previous transcriptional classification based on ASCL1, NeuroD1, and YAP1, thus providing limited mechanistic insight into the tumorigenesis. The reason for the discrepancy is unclear, but we did notice the overlap of several of these markers by IHC.

In summary, our results demonstrate the validity and importance of using both surgical and biopsy FFPE samples and serve as a valuable resource for the SCLC research community. This work should also help guide future pre-clinical investigations that seek more meaningful and efficacious stratification of SCLC in order to improve therapeutic responses and patient survival.

Materials and methods

Sample collection

Tumors in the discovery cohort (diagnosed from 2012 to 2018) were obtained with informed consent from archival sources at Tongji Hospital, Tongji Medical College, Huazhong University of Science and Technology, Wuhan, China. Tumors in the second cohort (diagnosed from 2018 to 2021) were biopsy samples obtained from the First Affiliated Hospital of Henan University, Kaifeng, China. The 52 samples in the ICI cohort was also from Tongji Hospital, Tongji Medical College, Huazhong University of Science and Technology (diagnosed from 2017 to 2021). The samples were collected from patients at initial diagnosis. All diagnoses were independently reviewed by three experienced pathologists, and complied with the latest World Health Organization classification standards. The tumors came from patients not treated with neoadjuvant chemotherapy or radiotherapy before operation, with no previous history of malignancy, having SCLC as the initial primary cancer diagnosis at the time of surgical resection, and with adequate tumor/tissue material as well as clinical annotation and follow-up time. The tumor cell content was $>$ 90% tumor cells judged by haematoxylin and eosin (H&E) staining and yielded $>$ 700 proteins in MS analysis. All cases were staged according to the National Comprehensive Cancer Network (NCCN) Clinical Practice Guidelines in Oncology for SCLC (version 4.2020).

IHC and assessment

Immunohistochemical staining was conducted using tissue arrays. Prior to deparaffinization, the slides were heated to 60°C for 10 min to melt the paraffin. The slides were then washed three times with xylene to solubilize and remove the paraffin. Next, the xylene was removed by washing three times with 100% ethanol followed by 75% ethanol, 50% ethanol, and phosphate buffer saline (PBS). After the sections were deparaffinized and hydrated, the endogenous peroxidase activity was blocked. Antigen retrieval was performed using the Dako Target Retrieval Solution, High pH (Catalog No. S1699, Agilent Technologies, Santa Clara, CA) on Dako Ominis (Agilent Technologies) at 98°C for 25 min. The slides were then incubated with the primary antibody at 4°C overnight.

Primary antibodies used in this study were: anti-ASCL1 antibody (1:200; Catalog No. ab211327, Abcam, Boston, MA), anti-NeuroD1 antibody (1:200; Catalog No. ab213725, Abcam), and anti-YAP1 antibody (1:50; Catalog No. ab52771, Abcam). After incubated with the secondary antibody of Universal SAP reagent kit (mouse/rabbit universal) (Catalog No. SAP-9100, Zhongshan Biotechnology, Beijing, China) for $\sim$ 1 h, the sections were visualized with the DAB kit (Catalog No. ZLI-9017, Zhongshan Biotechnology) and counterstained with hematoxylin. The stained samples were scored by three pathologists independently for the multiplication of staining intensity (1, weak; 2, moderate; 3, strong) and the percentage of positive tumor cells, which resulted in scores of 0–300. A score of $<$ 10 was designated as 0, 10–40 as 1+, 41–140 as 2+, and 141–300 as 3+. All samples with scores of $>$ 10 were considered positive cases.

Protein extraction, trypsin digestion, and liquid chromatography-tandem mass spectrometry processing

For each SCLC sample, proteins were extracted from three tissue slices (5-μm thick) from the FFPE block (2–5 mm in diameter). The deparaffinization procedure was the same as IHC as described above. Air dried sample was scraped from the slide and resolubilized in 100 ml of 50 mM NH_4HCO_3. The sample was then incubated at 95°C for 5 min for decrosslinking, and cooled to room temperature. Trypsin digestion was carried out at 37°C overnight. Peptides were extracted twice with 200 μl of extraction buffer (50% acetonitrile and 0.1% formic acid in water) with 15 min vortex. The resulting peptides were dried and stored at −80°C for future analysis. The digested peptides were eluted, divided into three fractions, and analyzed on a Q Exactive HF-X (Catalog No. 2151480, Thermo Fisher Scientific, Waltham, MA) or Orbitrap Exploris 480 Mass Spectrometer (Catalog No. BRE725539, Thermo Fisher Scientific) coupled with an UltiMate 3000 RSLCnano LC system (Catalog No. 5200.0356, Thermo Fisher Scientific) and operated at data-dependent aquisition mode. MS1 was measured in the Orbitrap at a resolution of 60,000 followed by tandem MS scans of the top 40 precursors using higher-energy collision dissociation with 27% of normalized collision energy and 15 s of dynamic exclusion time.

MS data analysis

MS raw files were searched against the National Center for Biotechnology Information (NCBI) RefSeq human proteome database (updated on 04/07/2013, 27,414 entries) in Firmiana [62], a one-stop proteomic cloud platform for data processing and analysis, implemented with Mascot search engine with Percolator (Matrix Science, version 2.3.01). The following search parameters were used: (1) mass tolerances were 20 ppm for precursor ions and 0.05 Da for product ions; (2) up to two missed cleavages were allowed; (3) the minimal peptide length was seven amino acids; (4) cysteine carbamidomethylation was set as a fixed modification, and N-acetylation and methionine oxidation were considered variable modifications; and (5) the charges of precursor ions were limited to +2, +3, +4, +5, and +6. The peptide and protein false discovery rates (FDRs) were both set to 1%. A label-free, intensity-based absolute quantification (iBAQ) algorithm was used for protein quantification. The iBAQ values were calculated by dividing the raw intensities by the number of theoretical observable peptides. FOT, calculated by dividing a protein's iBAQ by the sum of iBAQs of all identified proteins in a single experiment, was used as normalized abundance to compare protein abundance across all experiments. The missing value was imputed with 1/10 of the global non-zero minimum value of the sample [63].

Subtyping and validation

A NMF consensus clustering algorithm was used for subtyping the discovery dataset. The standard "brunet" option was selected and 50 iterations were performed. The number of clusters (k) was set as 2 to 6, and the minimum member of each subclass was set as 10. The silhouette indicator (average silhouette > 0.8) and prognostic association ($P < 0.01$) were used to determine the optimal clustering number.

To develop a robust classification model, we first selected the top 1100 most abundant proteins detected from each sample, which yielded a dataset of 3460 proteins; then the 445 proteins that were detected in at least 8 samples (> 10%) with the CV greater than 1.9 were used for NMF consensus clustering (Table S3).

To validate the classification in an independent external dataset, the RF classifier was implemented on the discovery dataset using the R package randomForest. The top 500 most abundant proteins detected in each sample were aggregated for differential expression analysis. Finally, 58 significantly differentially expressed proteins (FC > 1.5; adjusted t-test, $P < 0.05$) with high identification frequencies (detected in more than 25% of the samples) were used as input (predictor variables). The subtype terms of SCLC on the discovery dataset were used as the response variables. The optimal parameters were estimated from the R function training with package caret. The 10-fold cross-validation strategy was utilized for internal validation.

Survival analysis

The Kaplan–Meier method, log-rank test, and the Cox proportional-hazards model with Wald statistics were used for survival analysis in all datasets. The multivariate Cox analysis was adjusted for age, sex, staging system, and chemotherapy. HRs with 95% CI were estimated for each variable. All calculated P values were two-sided where $P < 0.05$ was considered statistically significant.

Bioinformatic analysis

To investigate the proteomic features of SCLC subtypes, we selected significantly altered proteins by comparing their expression in each subtype to the other subtypes (FC > 3 for S-I and S-II or FC > 10 for S-III; Wilcox test, $P < 0.05$). Metascape analysis was conducted online (https://metascape.org) for functional pathway analysis. The on-line tool SangerBox (http://www.sangerbox.com/tool.html) was used for generating the plots and heatmap. All other statistical analyses were carried out with R 3.6.1.

Ethical statement

This study was approved by the ethical committee of Tongji Hospital, Tongji Medical College, Huazhong University of Science and Technology, China (Approval No. TJ-IRB20201011). The written informed consent was obtained from the participating patients.

Data availability

All data and search results have been deposited to the iProX database (iProX: IPX0004230000), which are publicly accessible at http://www.iprox.org.

CRediT author statement

Zitian Huo: Writing – original draft, Formal analysis, Investigation, Visualization. **Yaqi Duan:** Writing – review & editing, Methodology. **Dongdong Zhan:** Investigation, Data curation, Validation. **Xizhen Xu:** Visualization, Writing – review & editing. **Nairen Zheng:** Data curation, Validation. **Jing Cai:** Data curation, Resources. **Ruifang Sun:** Resources, Data curation. **Jianping Wang:** Resources, Data curation. **Fang Cheng:** Resources, Data curation. **Zhan Gao:** Resources, Data curation. **Caixia Xu:** Resources, Data curation. **Wanlin Liu:** Resources, Data curation. **Yuting Dong:** Resources, Data curation. **Sailong Ma:** Resources. **Qian Zhang:** Resources. **Yiyun Zheng:** Resources. **Liping Lou:** Resources. **Dong Kuang:** Writing – review & editing. **Qian Chu:** Supervision, Project administration, Funding acquisition. **Jun Qin:** Conceptualization, Resources, Supervision, Project administration, Funding acquisition, Writing – review & editing. **Guoping Wang:** Conceptualization, Resources, Supervision, Project administration, Funding acquisition. **Yi Wang:** Conceptualization, Resources, Supervision, Project administration, Funding acquisition, Writing – review & editing. All authors have read and approved the final manuscript.

Supplementary material

Supplementary material is available at *Genomics, Proteomics & Bioinformatics* online (https://doi.org/10.1093/gpbjnl/qzae033).

Competing interests

Jun Qin and Yi Wang are cofounders and co-owners of the Beijing Pineal Diagnostics Co., Ltd., and Dongdong Zhan and Fang Cheng are employees of the Beijing Pineal Diagnostics Co., Ltd. All the other authors have declared no competing interests.

Acknowledgments

This work was supported by the National Key R&D Program of China (Grant Nos. 2018YFA0507503, 2017YFA0505102, 2017YFA0505103, and 2017YFA0505104), the National Natural Science Foundation of China (Grant Nos. 82072597, 62131009, 31770892, 31970725, 31870828, 81874237, and 81974016), the Beijing Municipal Natural Science Foundation (Grant No. 7192199), the State Key Laboratory of Proteomics (Grant No. SKLP-K202002), the Kaifeng Science and Technology Development Plan Project (Grant No. 1806005), China. We thank the Mass Spectrometry Platform of National Center for Protein Sciences (Beijing) (PHOENIX Center) for technical assistance. We also thank all the patients who participated in this study, as well as the clinicians and staff of the institutions who assisted with the studies.

ORCID

0000-0002-7368-0831 (Zitian Huo)
0000-0002-2392-5642 (Yaqi Duan)
0000-0002-0704-8782 (Dongdong Zhan)
0009-0000-3222-6862 (Xizhen Xu)
0000-0002-3952-1570 (Nairen Zheng)
0000-0001-8002-2645 (Jing Cai)

0000-0002-4791-3734 (Ruifang Sun)
0000-0001-6142-7153 (Jianping Wang)
0000-0001-9385-204X (Fang Cheng)
0009-0001-9697-6547 (Zhan Gao)
0009-0003-1014-1448 (Caixia Xu)
0000-0002-4116-2597 (Wanlin Liu)
0000-0003-0886-9221 (Yuting Dong)
0009-0007-5118-6991 (Sailong Ma)
0000-0002-0869-3951 (Qian Zhang)
0000-0001-8103-3688 (Yiyun Zheng)
0000-0002-9542-568X (Liping Lou)
0000-0001-9558-0333 (Dong Kuang)
0000-0001-8192-7630 (Qian Chu)
0000-0003-3769-3720 (Jun Qin)
0009-0000-6472-0849 (Guoping Wang)
0000-0002-2088-2085 (Yi Wang)

References

[1] Rudin CM, Durinck S, Stawiski EW, Poirier JT, Modrusan Z, Shames DS, et al. Comprehensive genomic analysis identifies *SOX2* as a frequently amplified gene in small-cell lung cancer. Nat Genet 2012;44:1111–6.
[2] George J, Lim JS, Jang SJ, Cun Y, Ozretić L, Kong G, et al. Comprehensive genomic profiles of small cell lung cancer. Nature 2015;524:47–53.
[3] Umemura S, Mimaki S, Makinoshima H, Tada S, Ishii G, Ohmatsu H, et al. Therapeutic priority of the PI3K/AKT/mTOR pathway in small cell lung cancers as revealed by a comprehensive genomic analysis. J Thorac Oncol 2014;9:1324–31.
[4] Rudin CM, Poirier JT, Byers LA, Dive C, Dowlati A, George J, et al. Molecular subtypes of small cell lung cancer: a synthesis of human and mouse model data. Nat Rev Cancer 2019;19:289–97.
[5] Gazdar AF, Bunn PA, Minna JD. Small-cell lung cancer: what we know, what we need to know and the path forward. Nat Rev Cancer 2017;17:725–37.
[6] Iams WT, Porter J, Horn L. Immunotherapeutic approaches for small-cell lung cancer. Nat Rev Clin Oncol 2020;17:300–12.
[7] Gazdar AF, Carney DN, Nau MM, Minna JD. Characterization of variant subclasses of cell lines derived from small cell lung cancer having distinctive biochemical, morphological, and growth properties. Cancer Res 1985;45:2924–30.
[8] Graziano SL, Cowan BY, Carney DN, Bryke CR, Mitter NS, Johnson BE, et al. Small cell lung cancer cell line derived from a primary tumor with a characteristic deletion of 3p. Cancer Res 1987;47:2148–55.
[9] Arvelo F, Poupon MF, Le Chevalier T. Establishment and characterization of five human small cell lung cancer cell lines from early tumor xenografts. Anticancer Res 1994;14:1893–901.
[10] Carney DN, Gazdar AF, Bepler G, Guccion JG, Marangos PJ, Moody TW, et al. Establishment and identification of small cell lung cancer cell lines having classic and variant features. Cancer Res 1985;45:2913–23.
[11] Borromeo MD, Savage TK, Kollipara RK, He M, Augustyn A, Osborne JK, et al. ASCL1 and NEUROD1 reveal heterogeneity in pulmonary neuroendocrine tumors and regulate distinct genetic programs. Cell Rep 2016;16:1259–72.
[12] Huang YH, Klingbeil O, He XY, Wu XS, Arun G, Lu B, et al. POU2F3 is a master regulator of a tuft cell-like variant of small cell lung cancer. Genes Dev 2018;32:915–28.
[13] Baine MK, Hsieh MS, Lai WV, Egger JV, Jungbluth AA, Daneshbod Y, et al. SCLC subtypes defined by ASCL1, NEUROD1, POU2F3, and YAP1: a comprehensive immunohistochemical and histopathologic characterization. J Thorac Oncol 2020;15:1823–35.
[14] Gay CM, Stewart CA, Park EM, Diao L, Groves SM, Heeke S, et al. Patterns of transcription factor programs and immune pathway activation define four major subtypes of SCLC with distinct therapeutic vulnerabilities. Cancer Cell 2021;39:346–60.e7.
[15] Paz-Ares L, Dvorkin M, Chen Y, Reinmuth N, Hotta K, Trukhin D, et al. Durvalumab plus platinum–etoposide versus platinum–etoposide in first-line treatment of extensive-stage small-cell lung cancer (CASPIAN): a randomised, controlled, open-label, phase 3 trial. Lancet 2019;394:1929–39.
[16] Chan JM, Quintanal-Villalonga Á, Gao VR, Xie Y, Allaj V, Chaudhary O, et al. Signatures of plasticity, metastasis, and immunosuppression in an atlas of human small cell lung cancer. Cancer Cell 2021;39:1479–96.e18.
[17] Ni X, Tan Z, Ding C, Zhang C, Song L, Yang S, et al. A region-resolved mucosa proteome of the human stomach. Nat Commun 2019;10:39.
[18] Mun DG, Bhin J, Kim S, Kim H, Jung JH, Jung Y, et al. Proteogenomic characterization of human early-onset gastric cancer. Cancer Cell 2019;35:111–24.e10.
[19] Jiang Y, Sun A, Zhao Y, Ying W, Sun H, Yang X, et al. Proteomics identifies new therapeutic targets of early-stage hepatocellular carcinoma. Nature 2019;567:257–61.
[20] Gao Q, Zhu H, Dong L, Shi W, Chen R, Song Z, et al. Integrated proteogenomic characterization of HBV-related hepatocellular carcinoma. Cell 2019;179:561–77.e22.
[21] Shrestha R, Llaurado Fernandez M, Dawson A, Hoenisch J, Volik S, Lin YY, et al. Multiomics characterization of low-grade serous ovarian carcinoma identifies potential biomarkers of MEK inhibitor sensitivity and therapeutic vulnerability. Cancer Res 2021;81:1681–94.
[22] Li C, Sun YD, Yu GY, Cui JR, Lou Z, Zhang H, et al. Integrated omics of metastatic colorectal cancer. Cancer Cell 2020;38:734–47.e9.
[23] Zhan D, Zheng N, Zhao B, Cheng F, Tang Q, Liu X, et al. Expanding individualized therapeutic options via genoproteomics. Cancer Lett 2023;560:216123.
[24] Gillette MA, Satpathy S, Cao S, Dhanasekaran SM, Vasaikar SV, Krug K, et al. Proteogenomic characterization reveals therapeutic vulnerabilities in lung adenocarcinoma. Cell 2020;182:200–25.e35.
[25] Ge S, Xia X, Ding C, Zhen B, Zhou Q, Feng J, et al. A proteomic landscape of diffuse-type gastric cancer. Nat Commun 2018;9:1012.
[26] Ganti AKP, Loo BW, Bassetti M, Blakely C, Chiang A, D'Amico TA, et al. Small cell lung cancer, version 2.2022, NCCN clinical practice guidelines in oncology. J Natl Compr Canc Netw 2021;19:1441–64.
[27] Fischbach H, Döring M, Nikles D, Lehnert E, Baldauf C, Kalinke U, et al. Ultrasensitive quantification of TAP-dependent antigen compartmentalization in scarce primary immune cell subsets. Nat Commun 2015;6:6199.
[28] Palomar G, Dudek K, Wielstra B, Jockusch EL, Vinkler M, Arntzen JW, et al. Molecular evolution of antigen-processing genes in salamanders: do they coevolve with MHC class I genes? Genome Biol Evol 2021;13:evaa259.
[29] Leverson JD, Sampath D, Souers AJ, Rosenberg SH, Fairbrother WJ, Amiot M, et al. Found in translation: how preclinical research is guiding the clinical development of the BCL2-selective inhibitor venetoclax. Cancer Discov 2017;7:1376–93.
[30] Duan R, Du W, Guo W. EZH2: a novel target for cancer treatment. J Hematol Oncol 2020;13:104.
[31] Petersen SL, Chen TT, Lawrence DA, Marsters SA, Gonzalvez F, Ashkenazi A. TRAF2 is a biologically important necroptosis suppressor. Cell Death Differ 2015;22:1846–57.
[32] Cheng Y, Han L, Wu L, Chen J, Sun H, Wen G, et al. Effect of first-line serplulimab *vs* placebo added to chemotherapy on survival in patients with extensive-stage small cell lung cancer: the ASTRUM-005 randomized clinical trial. JAMA 2022;328:1223–32.

[33] El Sayed R, Blais N. Immunotherapy in extensive-stage small cell lung cancer. Curr Oncol 2021;28:4093–108.
[34] Gardner EE, Lok BH, Schneeberger VE, Desmeules P, Miles LA, Arnold PK, et al. Chemosensitive relapse in small cell lung cancer proceeds through an EZH2–SLFN11 axis. Cancer Cell 2017; 31:286–99.
[35] Leslie M. First EZH2 inhibitor approved-for rare sarcoma. Cancer Discov 2020;10:333–4.
[36] Zhou L, Mudianto T, Ma X, Riley R, Uppaluri R. Targeting EZH2 enhances antigen presentation, antitumor immunity, and circumvents anti-PD-1 resistance in head and neck cancer. Clin Cancer Res 2020;26:290–300.
[37] Moore AM, Einhorn LH, Estes D, Govindan R, Axelson J, Vinson J, et al. Gefitinib in patients with chemo-sensitive and chemo-refractory relapsed small cell cancers: a Hoosier Oncology Group phase II trial. Lung Cancer 2006;52:93–7.
[38] Arnold D, Lueza B, Douillard JY, Peeters M, Lenz HJ, Venook A, et al. Prognostic and predictive value of primary tumour side in patients with RAS wild-type metastatic colorectal cancer treated with chemotherapy and EGFR directed antibodies in six randomized trials. Ann Oncol 2017;28:1713–29.
[39] Mak DWS, Li S, Minchom A. Challenging the recalcitrant disease-developing molecularly driven treatments for small cell lung cancer. Eur J Cancer 2019;119:132–50.
[40] Held L, Siu C, Shadman M. Venetoclax as a therapeutic option for the treatment of chronic lymphocytic leukemia: the evidence so far. Expert Opin Pharmacother 2021;22:655–65.
[41] Lochmann TL, Floros KV, Naseri M, Powell KM, Cook W, March RJ, et al. Venetoclax is effective in small-cell lung cancers with high BCL-2 expression. Clin Cancer Res 2018;24:360–9.
[42] Liewer S, Huddleston A. Alisertib: a review of pharmacokinetics, efficacy and toxicity in patients with hematologic malignancies and solid tumors. Expert Opin Investig Drugs 2018;27:105–12.
[43] Vénéreau E, Ceriotti C, Bianchi ME. DAMPs from cell death to new life. Front Immunol. 2015;6:422.
[44] Sprooten J, De Wijngaert P, Vanmeerbeerk I, Martin S, Vangheluwe P, Schlenner S, et al. Necroptosis in immuno-oncology and cancer immunotherapy. Cells 2020;9:1823.
[45] Bist P, Leow SC, Phua QH, Shu S, Zhuang Q, Loh WT, et al. Annexin-1 interacts with NEMO and RIP1 to constitutively activate IKK complex and NF-κB: implication in breast cancer metastasis. Oncogene 2011;30:3174–85.
[46] Park S, Hatanpaa KJ, Xie Y, Mickey BE, Madden CJ, Raisanen JM, et al. The receptor interacting protein 1 inhibits p53 induction through NF-κB activation and confers a worse prognosis in glioblastoma. Cancer Res 2009;69:2809–16.
[47] McCormick KD, Ghosh A, Trivedi S, Wang L, Coyne CB, Ferris RL, et al. Innate immune signaling through differential RIPK1 expression promote tumor progression in head and neck squamous cell carcinoma. Carcinogenesis 2016;37:522–9.
[48] Li X, Guo J, Ding AP, Qi WW, Zhang PH, Lv J, et al. Association of mixed lineage kinase domain-like protein expression with prognosis in patients with colon cancer. Technol Cancer Res Treat 2017;16:428–34.
[49] Li L, Yu S, Zang C. Low necroptosis process predicts poor treatment outcome of human papillomavirus positive cervical cancers by decreasing tumor-associated macrophages M1 polarization. Gynecol Obstet Invest 2018;83:259–67.
[50] He L, Peng K, Liu Y, Xiong J, Zhu FF. Low expression of mixed lineage kinase domain-like protein is associated with poor prognosis in ovarian cancer patients. Onco Targets Ther 2013;6:1539–43.
[51] Colbert LE, Fisher SB, Hardy CW, Hall WA, Saka B, Shelton JW, et al. Pronecrotic mixed lineage kinase domain-like protein expression is a prognostic biomarker in patients with early-stage resected pancreatic adenocarcinoma. Cancer 2013;119:3148–55.
[52] Jiao D, Cai Z, Choksi S, Ma D, Choe M, Kwon HJ, et al. Necroptosis of tumor cells leads to tumor necrosis and promotes tumor metastasis. Cell Res 2018;28:868–70.
[53] Ruan J, Mei L, Zhu Q, Shi G, Wang H. Mixed lineage kinase domain-like protein is a prognostic biomarker for cervical squamous cell cancer. Int J Clin Exp Pathol 2015;8:15035–8.
[54] Zhai E, Chen J, Wang K, Ye Z, Wu H, Chen C, et al. Prognostic value of mixed lineage kinase domain-like protein expression in the survival of patients with gastric caner. Tumour Biol 2016; 37:13679–85.
[55] Yang C, Sengupta S, Hegde PM, Mitra J, Jiang S, Holey B, et al. Regulation of oxidized base damage repair by chromatin assembly factor 1 subunit A. Nucleic Acids Res 2017;45:739–48.
[56] Nera B, Huang HS, Lai T, Xu L. Elevated levels of TRF2 induce telomeric ultrafine anaphase bridges and rapid telomere deletions. Nat Commun 2015;6:10132.
[57] Lee JH, You J, Dobrota E, Skalnik DG. Identification and characterization of a novel human PP1 phosphatase complex. J Biol Chem 2010;285:24466–76.
[58] Nayak A, Dutta M, Roychowdhury A. Emerging oncogene ATAD2: signaling cascades and therapeutic initiatives. Life Sci 2021;276:119322.
[59] Burrell RA, McClelland SE, Endesfelder D, Groth P, Weller MC, Shaikh N, et al. Replication stress links structural and numerical cancer chromosomal instability. Nature 2013;494:492–6.
[60] Feng W, Yonezawa M, Ye J, Jenuwein T, Grummt I. PHF8 activates transcription of rRNA genes through H3K4me3 binding and H3K9me1/2 demethylation. Nat Struct Mol Biol 2010; 17:445–50.
[61] Lee YC, Kim YJ. Requirement for a functional interaction between mediator components Med6 and Srb4 in RNA polymerase II transcription. Mol Cell Biol 1998;18:5364–70.
[62] Feng J, Ding C, Qiu N, Ni X, Zhan D, Liu W, et al. Firmiana: towards a one-stop proteomic cloud platform for data processing and analysis. Nat Biotechnol 2017;35:409–12.
[63] Huang W, Zhan D, Li Y, Zheng N, Wei X, Bai B, et al. Proteomics provides individualized options of precision medicine for patients with gastric cancer. Sci China Life Sci 2021; 64:1199–211.

Genomics, Proteomics & Bioinformatics, 2024, 22, 1–12
https://doi.org/10.1093/gpbjnl/qzae033
Original Research